J. Cent. South Univ. (2015) 22: 610−618
DOI: 10.1007/s11771-015-2562-2

Springer

Evaluation of nitrate source in groundwater of southern part of North China Plain based on multi-isotope

FANG Jing-jing(方晶晶), ZHOU Ai-guo(周爱国), MA Chuan-ming(马传明), LIU Cun-fu(刘存富),
CAI He-sheng(蔡鹤生), GAN Yi-qun(甘义群), LIU Yun-de(刘运德)

School of Environmental Studies & State Key Laboratory of Biogeology and Environmental Geology,
China University of Geosciences, Wuhan 430074, China

Abstract: Nitrate pollution in groundwater is a serious water quality problem that increases the risk of developing various cancers. Groundwater is the most important water resource and supports a population of 5 million in Anyang area of the southern part of the North China Plain. Determining the source of nitrate pollution is the challenge in hydrology area due to the complex processes of migration and transformation. A new method is presented to determine the source of nitrogen pollution by combining the composition characteristics of stable carbon isotope in dissolved organic carbon in groundwater. The source of groundwater nitrate is dominated by agricultural fertilizers, as well as manure and wastewater. Mineralization, nitrification and mixing processes occur in the groundwater recharge area, whereas the confined groundwater area is dominated by denitrification processes.

Key words: $\delta^{15}N_{NO_3}$;$\delta^{18}O_{NO_3}$; $\delta^{13}C_{DOC}$; esophageal cancer; groundwater

1 Introduction

The nitrate pollution in groundwater is one of the most prevalent water environmental problems in the worldwide [1], increasing the risk of many cancers including colon cancer, esophageal caner, and etc. It can be originated from multiple sources, including the excess application of mineral N fertilizers, animal manure in agriculture, discharges from urban or industrial N, and etc. To determine the sources of the nitrate pollution, several measures have been applied in the past 40 years by separately considering the stable isotope ratio of nitrogen ($\delta^{15}N_{NO_3}$) and oxygen ($\delta^{18}O_{NO_3}$) in nitrate [2−9]. The mean mass concentration of NO_3^- in the groundwater in the studied industrial areas or in the residential areas exceeds the Drinking Water Regulations of European Communities guide mass concentration of 25 mg/L [10]. Recently, the nitrate isotope tracer method was developed to estimate the pollution sources by isotopic comparison between the water samples and possible source materials. Although this isotopic comparison has been as a denitrification indicator by analyzing isotopic enrichment trends of water samples [11], the problem of identifying nitrate pollution sources is still unsolved, due to the fact that source materials in nitrate pollution (e.g. manure and sewage) usually have a similar isotope signature, and there is isotopic compositions overlap between the source characteristics and denitrification similar trends. Therefore, there is a great need of developing new approach to effectively identify the sources of nitrate pollution.

In this work, we first investigated the distribution of $\delta^{15}N_{NO_3}$,$\delta^{18}O_{NO_3}$ and $\delta^{13}C_{DOC}$ in the groundwater of the Anyang area, China. Traditional geochemical and isotope parameters, such as total dissolved solids (TDS) concentrations, dissolved organic carbon (DOC) concentrations, δD and $\delta^{18}O$ of groundwater (δD and $\delta^{18}O_{H_2O}$), and the coliform bacteria, were also measured. We attempted to identify NO_3^- sources for groundwater and address what dominantly controls $\delta^{15}N_{NO_3}$ and $\delta^{18}O_{NO_3}$ in the groundwater of the Anyang area, China.

Discriminating multiple NO_3^- sources by their N isotopic composition alone is impossible whenever heterogenic or autogenic denitrification occurs. Thus, there is a need for establishing co-migrating discriminators of NO_3^- sources. The N and C isotope compositions have been used to identify the pollution sources, the formation mechanism, and migration characteristics of nitrate.

2 Study site

Anyang area, located at 113°37′E and 114°58′E and 35°12′N and 36°22′N [12], is bordered by the Taihang

---

Foundation item: Projects(41072179, 41002083) supported by the National Natural Science Foundation of China
Received date: 2013−11−07; **Accepted date:** 2014−09−12
Corresponding author: ZHOU Ai-guo, Professor, PhD; Tel.: +86−27−67883060; E-mail: aiguozhou@cug.edu.cn

Mountains of the west and the Zhanghe River to the north, by the Puyang city to the east and the Hebi and Xinxiang city to the south (Fig. 1). The terrain slopes from west to east, and the elevation above sea level is 1632−48.4 m. The Anyang area is under middle-latitude continental semi-arid monsoon climate, with mean annual temperature of 12.5–14.6 °C and mean annual precipitation and potential evaporation of 606.1 mm and of 1584.3−2335.3 mm, respectively. The atmospheric precipitation is dominated by the Asia summer monsoon.

The main river of the study area is Anyang River with a total length of 147 km, which belongs to the Wei River of Haihe River Basin and originated from the Qingquan village in Linzhou. The river water comes from atmospheric precipitation and karst springs, and is a perennial river that flows from west to east, with an average annual runoff of 3.76×10^6 m^3, the general flow of 8 m^3/s, dry season flow of 6 m^3/s and the flood maximum flow rate of 2060 m^3/s.

Detailed hydraulic and hydrochemical studies have been investigated in the study area. The regional quaternary groundwater is divided into four part connected aquifers, which is karst fractured aquifer, bedrock fractured aquifer, clastic rock pore and fractured aquifer, and loose sand pore aquifer, respectively (Fig. 2). The quaternary aquifers consist of sandy gravel, medium-fine and fine grained sand and are separated by a sequence of silt and clay layers considered aquitards or aquifuges [8].

3 Groundwater sampling and analytical methods

Groundwater samples were collected out of 38 wells in 2010 in the study area (Fig. 1). In addition to the spring water and surface water, all wells are used for drinking water or irrigation. The wells depths of the quaternary groundwater range from 6 to 200 m along the Zhenzhu spring river and from 15 to 200 m along the Xiaonanhai spring river. Water samples were collected from active pumping wells used either for domestic, industrial, or agricultural purposes, and were initially preserved in a cold box and later transferred to a refrigerator in the laboratory. The temperature and pH of groundwater were measured on site at the wellhead, and alkalinity was determined by titration within 24 h after sampling. Samples were filtered with 0.45 μm membrane filters for measurement of ion concentrations and isotopic compositions. The concentrations of major cations and anions were measured by inductively coupled plasma-optical emission spectrometry (ICP-OES) and ion chromatography (IC), respectively. Ion charge imbalances are within ±5%. Dissolved organic carbon (DOC) concentrations of groundwater were measured using an AnalytikJena AG TOC/TN analyzer at the Analysis Laboratory of Institute of Chemistry and Materials Science, University for Nationalities. The bacteriaum E.coli, which is the indicator of manure contamination, was determinated by the coliform

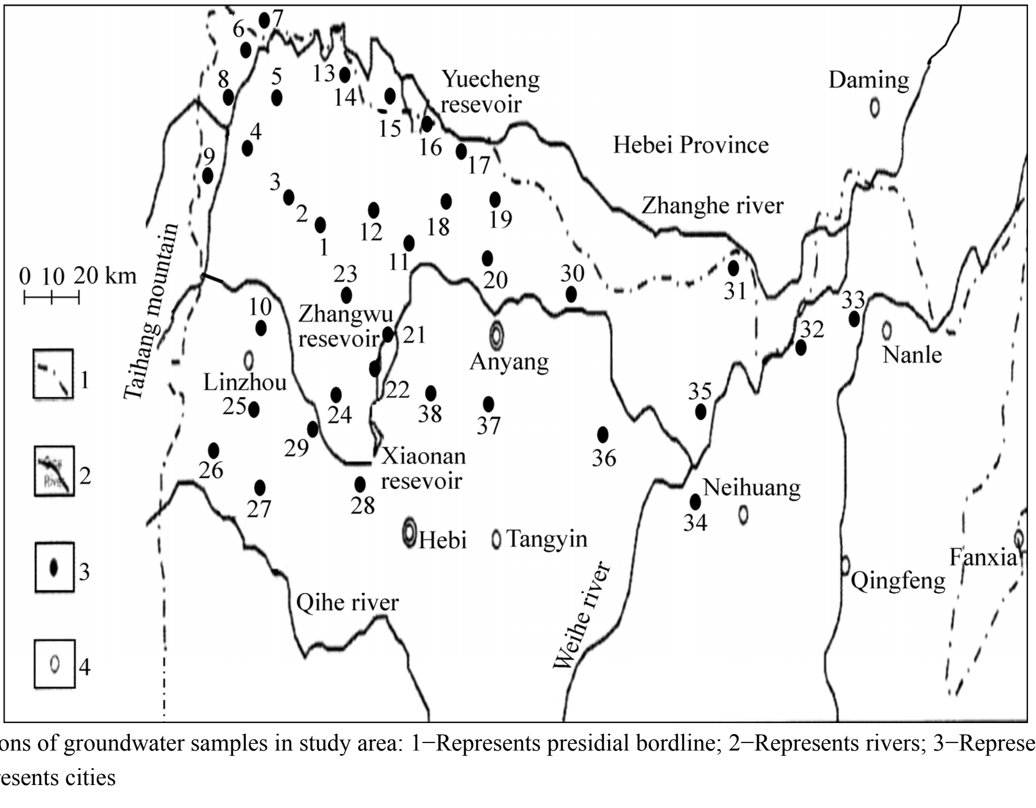

Fig. 1 Locations of groundwater samples in study area: 1−Represents presidial bordline; 2−Represents rivers; 3−Represents sampling sites; 4−Represents cities

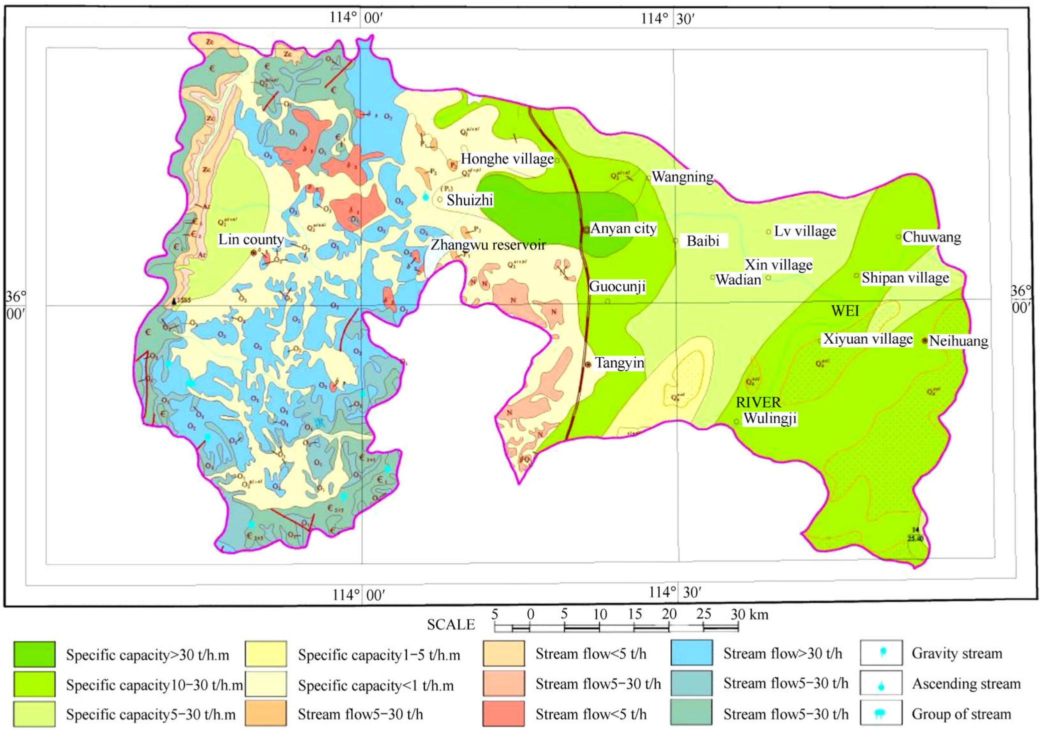

Fig. 2 Map of hydrogeological divisions in study area

bacteria test method. The maximum probability of bacteria E.coli was calculated using the U.S EPA-validated tools and standards of business incubators. The water samples need to be added to the medium for 24 h of incubation at 350 °C in the incubation, and the bacteria were observed and counted. 1−2 sterile water samples were used to be analyzed for each batch of samples.

Stable isotope ratios are reported in parts per thousand (‰) using the conventional delta notation: $\delta_{\text{sample}}=[(R_{\text{sample}}-R_{\text{standard}})/R_{\text{standard}}]\times 1000‰$, where R represents the ^{18}O/^{16}O, or ^{2}H/^{1}H ratios of the samples and standards, respectively. $\delta^{18}O_{H_2O}$ and δD were determined at the State Key Laboratory of Biogeology and Environmental Geology, China University of Geosciences (CUG), using online thermal conversion elemental analysis isotope ratio mass spectrometry (TC/EA-IRMS) method. The precisions of measurements are ±0.1‰ and ±1‰, respectively, and results are reported relative to V-SMOW.

For $\delta^{13}C_{\text{DOC}}$ analysis, water samples were concentrated to 3−4 mL at 40 °C by rotary evaporation then brought to pH 2 by adding 2−3 drops of 85% phosphoric acid by removing the dissolved inorganic carbon (DIC) under agitation. After drying at 70 °C, the samples which were loaded to the autosampler of elemental analyzer (EA) instantaneously combusted in the enriched reaction tube at 1020 °C. The $\delta^{13}C_{\text{DOC}}$ value was determined via CO_2 carried by He gas to IRMS, and the test precision was better than 0.2‰.

In the field, 1−5 L samples were collected to ensure 80−100 mg of nitrate on the cation exchange resin. The samples which were concentrated to 300 mL were taken through the activated carbon in order to remove the dissolved organic carbon. After removing SO_4^{2-} by addition of $BaCl_2$ to 300 mL water, the water was carried through the cation exchange resin, and a flow rate of 2−5 mL/min is achieved by adjusting the stopcock on the separatory funnel. The KNO_3 and KCl solutions were produced by adding 1 mol/L KOH solution eluent to neutral, and were dried at 90 °C. $\delta^{15}N_{NO_3}$ and $\delta^{18}O_{NO_3}$ were determined at the same time in one sample input using online high-temperature pyrolysis of 500 μg KNO_3. N_2 and CO generated by KNO_3 and C reaction were separated through the chromatographic column at 60 °C coupled with ConFloⅣ and IRMS, and the precisions of δ^{15}N and δ^{18}O were 0.25‰ and 0.6‰, respectively, compared with that of 0.1‰ and 0.5‰ abroad.

4 Results

4.1 Chemical compositions of groundwater

The chemical and isotopic compositions of the groundwater are listed in Tables 1 and 2, respectively.

The karst water samples indicated predominantly HCO_3−Ca−Mg type water, while HN026 was corresponding to a SO_4−HCO_3−Ca−Mg type, with temperatures ranging from 17.0 to 28.6 ° C, pH from 6.69 to 8.17, the TDS concentrations from 219.7 to

Table 1 Chemical compositions and field data of groundwater in study area

Sample ID	Depth/ m	Type of groundwater	t/°C	pH	Mass concentrations/(mg·L^{-1})										Chemical type
					TDS	HCO_3^-	Cl^-	SO_4^{2-}	NO_3^-	K^+	Na^+	Ca^{2+}	Mg^{2+}	DOC	
HN001	120	Karst water	17.0	7.43	335.0	269.7	16.1	48.7	22.80	3.4	8.3	80.8	19.1	3.94	HCO_3–Ca–Mg
HN002	120	Karst water	22.8	8.06	303.6	230.0	15.9	51.1	24.80	3.5	8.6	71.1	17.9	4.66	HCO_3–Ca–Mg
HN003	160	Karst water	24.6	7.36	497.1	237.9	41.5	105.1	44.21	3.5	18.3	119.4	24.3	8.32	HCO_3–SO_4–Ca
HN005	185	Karst water	21.0	7.52	432.5	253.8	28.2	66.5	51.60	3.6	10.2	103.6	31.9	7.81	HCO_3–Ca–Mg
HN014	200	Karst water	23.7	7.88	344.5	269.7	17.0	60.8	18.50	3.9	12.2	70.6	27.3	5.66	HCO_3–Ca–Mg
HN019	200	Karst water	23.8	6.69	523.9	444.2	38.4	44.6	44.94	3.4	34.3	100.3	28.2	6.27	HCO_3–Ca–Mg
HN023	200	Karst water	24.1	7.76	328.9	269.7	16.7	42.0	40.08	3.6	7.0	80.6	19.4	4.05	HCO_3–Ca–Mg
HN024	200	Karst water	22.1	7.86	320.4	269.7	16.5	36.5	29.85	3.7	6.8	82.6	18.3	3.58	HCO_3–Ca–Mg
HN025	170	Karst water	28.6	7.58	219.7	206.2	16.0	31.3	23.50	3.6	2.1	28.6	11.5	—	HCO_3–Ca–Mg
HN026	180	Karst water	20.7	8.17	268.9	158.7	23.6	75.4	24.80	4.4	15.3	51.7	18.9	—	SO_4–HCO_3–Ca–Mg
HN027	185	Karst water	18.6	7.75	344.0	253.8	20.0	51.1	30.30	3.6	8.4	83.1	20.3	—	HCO_3–Ca–Mg
HN028	190	Karst water	21.3	7.62	335.1	269.7	20.9	42.0	24.70	3.8	6.8	83.7	18.3	—	HCO_3–Ca–Mg
HN004	25	Pore water	21.6	7.62	282.1	269.7	13.4	18.7	27.52	3.4	5.3	69.7	18.7	13.02	HCO_3–Ca–Mg
HN010	15	Pore water	21.6	7.47	645.3	301.4	191.6	55.4	43.49	3.1	9.8	189.9	44.8	3.34	HCO_3–Cl–Ca–Mg
HN011	40	Pore water	17.0	7.00	680.9	412.5	87.4	128.7	41.54	3.2	30.5	193.8	31	6.24	SO_4–HCO_3–Ca
HN013	15	Pore water	16.4	7.14	1582.3	364.9	89.1	820.6	89.26	3.4	158.8	291.9	36	5.91	HCO_3–SO_4–Ca–Mg
HN015	6	Pore water	16.2	7.05	816.5	396.6	146.5	165.8	75.47	4.2	41.3	232.4	27.9	5.36	SO_4–Cl–HCO_3–Ca
HN016	10	Pore water	20.7	7.62	341.8	253.8	23.1	46.2	34.89	3.7	12.5	89.4	14.1	4.16	HCO_3–Ca
HN017	40	Pore water	20.2	7.30	589.5	285.6	37.9	182.8	25.83	3.6	17.7	142.5	28.1	5.36	SO_4–HCO_3–Ca–Mg
HN018	19	Pore water	17.1	7.30	612.8	285.6	85.3	104.6	98.17	3.6	33.8	138.1	23.6	8.83	SO_4–Cl–HCO_3–Ca
HN020	70	Pore water	21.7	9.14	679.3	317.3	130.4	110.3	52.60	3.6	29.1	163.9	30.7	5.49	HCO_3–Cl–Ca–Mg
HN029	17	Pore water	22.5	7.74	288.2	238.0	17.6	42.3	4.60	3.8	8.0	79.1	18.4	—	HCO_3–Ca–Mg
HN030	30	Pore water	22.2	7.74	412.3	364.9	48.7	42.7	21.57	3.9	92.0	28.0	20.6	6.48	HCO_3–Ca–Mg
HN031	40	Pore water	14.5	7.46	595.3	349.0	85.3	136.2	24.86	3.5	41.8	109.2	44.8	5.40	SO_4–Cl–HCO_3–Ca
HN032	70	Pore water	22.4	7.41	762.3	444.2	154.8	151.6	14.00	3.6	70.4	77.6	82.2	15.91	SO_4–Cl–HCO_3–Ca
HN033	35	Pore water	21.2	8.07	994.1	269.7	291.5	268.0	5.60	3.8	188.3	51.5	56.1	—	SO_4–Cl–HCO_3–Ca
HN034	40	Pore water	16.6	7.38	791.7	713.9	105.5	56.5	15.15	3.8	79.6	115.1	74.2	13.23	HCO_3–Ca–Mg
HN035	40	Pore water	18.2	7.30	457.7	491.8	29.4	20.0	22.04	3.7	33.8	79.3	40.2	9.22	HCO_3–Ca–Mg
HN036	12	Pore water	15.4	7.15	890.8	476.0	150.8	165.2	72.16	3.6	65.0	177.1	91.1	7.46	HCO_3–Cl–Ca–Mg
HN037	20	Pore water	24.6	7.65	380.4	269.7	33.1	40.4	44.40	3.7	12.7	97.8	13.3	5.93	HCO_3–Ca
HN038	70	Pore water	22.2	8.01	1585.2	253.8	52.6	61.8	57.43	4.8	28.6	96.6	16.2	7.54	HCO_3–Ca
HN007	Spring water	Spring water	20.5	8.23	325.4	174.5	10.6	103.5	22.00	3.5	3.1	71.4	24.0	4.06	HCO_3–Ca–Mg
HN008	Spring water	Spring water	18.2	7.81	338.4	237.9	10.5	78.6	21.86	3.5	3.2	72.9	20.2	10.55	HCO_3–Ca–Mg
HN009	Spring water	Spring water	19.2	8.21	276.8	206.2	8.6	66.0	19.87	3.5	2.1	62.4	19.7	7.78	HCO_3–Ca–Mg
HN012	Spring water	Spring water	18.8	7.5	333.3	317.3	14.9	39.3	19.00	3.3	6.5	72.1	20.5	4.23	HCO_3–Ca–Mg
HN021	Spring water	Spring water	16.1	7.56	314.9	253.8	22.3	57.7	19.09	3.8	11.3	81.3	19.8	7.16	HCO_3–Ca–Mg
HN006	Canal water	Canal water	22.1	7.15	505.5	222.1	52.1	141.8	38.60	4.1	40.6	93.5	23.4	13.51	HCO_3–Ca–Mg
HN022	130	Igneous rock	23.2	7.51	609.9	238.0	15.7	270.2	21.61	3.5	7.9	168.8	24.7	11.11	SO_4–HCO_3–Ca

Table 2 Isotopic compositions of groundwater in study area

Sample ID	δ^{18}O (vs. VSMOW)/‰	δ^{2}H (vs. VSMOW)/‰	$\delta^{13}C_{DOC}$ (vs. VPDB)/‰	δ^{15}N (vs. Air)/‰	$\delta^{18}O_{NO_3}$ (vs. VSMOW)/‰
HN001	−8.06	−60.7	−29.65	7.87	21.57
HN002	−8.36	−62.6	−26.42	4.90	15.39
HN003	−7.47	−58.6	−25.4	8.80	24.96
HN004	−8.22	−63.0	−26.41	4.67	8.20
HN005	−7.91	−61.7	−26.44	7.24	24.79
HN006	−7.80	−62.0	−32.39	11.86	21.60
HN007	−8.78	−64.5	−25.8	—	—
HN008	−8.43	−61.3	−26.09	−0.66	19.37
HN009	−9.59	−65.9	−24.78	−0.94	15.87
HN010	−7.81	−58.4	−26.48	7.44	13.82
HN011	−7.55	−57.4	−31.69	5.66	23.69
HN012	−8.31	−64.1	23.72	5.44	4.06
HN013	−7.74	−60.8	−26.69	6.32	13.50
HN014	−8.27	−63.4	−24.15	6.20	32.18
HN015	−7.16	−54.4	−26.32	12.00	12.93
HN016	−7.64	−61.2	−23.17	2.61	25.08
HN017	−7.52	−58.8	−27.63	7.32	9.37
HN018	−7.97	−61.2	−22.89	8.09	21.34
HN019	−8.41	−66.9	−28.97	12.88	35.85
HN020	−7.61	−60.0	−29.85	8.70	25.42
HN021	−7.89	−62.6	−25.40	7.00	48.03
HN022	−8.41	−62.2	−25.20	1.75	25.03
HN023	−8.32	−63.0	−25.57	4.94	39.55
HN024	−8.33	−62.2	−22.84	6.90	26.63
HN025	−8.50	−64.2	—	—	—
HN026	−7.92	−61.0	—	—	—
HN027	−8.41	−63.0	—	—	—
HN028	−8.47	−63.4	—	—	—
HN029	−9.12	−66.1	—	—	—
HN030	−10.00	−75.6	−24.54	8.14	19.34
HN031	−7.28	−56.0	−29.07	22.35	50.96
HN032	−8.69	−66.3	−30.24	—	22.45
HN033	−9.20	−71.1	—	—	—
HN034	−8.30	−63.0	−22.39	5.02	1.88
HN035	−8.16	−61.6	−30.15	10.19	36.91
HN036	−7.20	−56.8	−30.56	19.78	36.64
HN037	−7.70	−61.5	−31.62	—	—
HN038	−8.33	−64.6	−25.36	8.86	20.69

523.9 mg/L, and with Cl^- mass concentrations between 15.9 and 41.5 mg/L.

The quaternary pore water indicated a HCO_3−Ca−Mg, HCO_3−Cl−Ca−Mg, SO_4−HCO_3−Ca, HCO_3−SO_4−Ca−Mg, SO_4−Cl−HCO_3−Ca or SO_4−HCO_3−Ca−Mg type water with temperatures ranging from 14.5 to 24.6 °C, pH from 7.0 to 9.14, the TDS mass concentration from 282.1 to 1585.2 mg/L, and the highest Cl^- MASS concentration was up to 291.5 mg/L.

The spring mainly distributed in the western mountains. The major hydrochemical type was HCO_3−Ca−Mg, with higher temperature of approximately

20 °C, pH of 7.5−8.23. The TDS mass concentrations of these samples were less than 500 mg/L, with the Cl^- mass concentration from 8.6 to 22.3 mg/L.

4.2 Isotope compositions of water

As shown in Table 2, the δD values ranged from −66.9‰ to −58.6‰ for karst water with a median value of −62.56‰, while the $\delta^{18}O_{H_2O}$ values ranged from −8.5‰ to −7.74‰ with a median value of −8.20‰. The isotopic compositions of the quaternary pore water ranged from −75.6‰ to −54.4‰ for δD and from −10‰ to −7.16‰. Specifically, the δD and $\delta^{18}O_{H_2O}$ values of the springs ranged from −65.9‰ to −61.3‰ and −9.59‰ to −7.89‰, respectively. The δD and $\delta^{18}O_{H_2O}$ values scattered close to Global Meteoric Water Line (GMWL) of CRAIG [13], China Meteoric Water Line (CMWL) defined by ZHENG et al [14] and China Meteoric Water Line (CMWL) (Fig. 3), suggesting that the groundwater was primarily derived from rain. The lighter isotopic values in the karst water indicated that the mean altitude of the recharge area is higher whereas more enriched isotopic signatures indicate waters originated from the local water flow system. Possible evaporation effects on the quaternary pore water were accounted by the trend line.

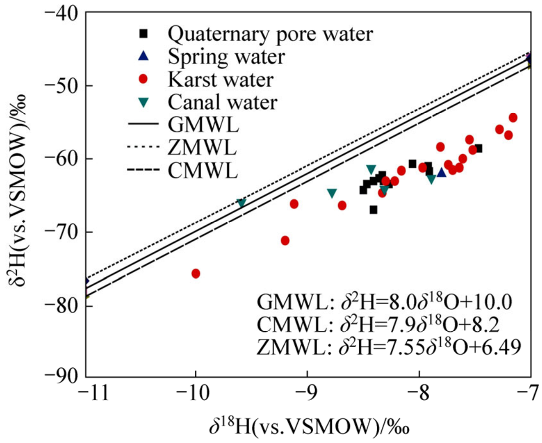

Fig. 3 Relationship between δ^{18}O and δ^2H values of groundwater samples from study area (GMWL refers to Global Meteoric Water Line of CRAIG [13]: $\delta^2H=8\delta^{18}O+10$; CMWL represents China Meteoric Water Line of ZHENG et al [14]: $\delta^2H=7.9\delta^{18}O+8.2$; ZMWL refers to Zhengzhou Meteoric Water Line: $\delta^2H=7.55\delta^{18}O+6.49$

4.3 Concentration and isotopic compositions of HO_3^-

The mass concentrations of HO_3^- in the karst water ranged from 18.5 to 51.6 mg/L, with the mean value of 31.7 mg/L. In addition, the range of HO_3^- in the quaternary pore water was from 4.6 to 98.17 mg/L with the mean value of 40.56 mg/L, which was generally higher than that of the karst water. The mean HO_3^- value in the spring water of this WORK was 20.36 mg/L, which was lower than the mean value of nitrate in the karst water.

The isotopic compositions of the HO_3^- in the karst water were found to range from 4.94‰ to 12.88‰ (mean 7.47‰) for δ^{15}N and from 15.39‰ to 39.55‰ (mean 27.62‰) for δ^{18}O, while for the quaternary pore water, the $\delta^{15}N_{NO_3}$ values range from 2.61‰ to 22.35‰ (mean 9.14‰) with the $\delta^{18}O_{NO_3}$ values of 1.88‰ to 50.96‰ (mean 21.39‰), for the spring water, the $\delta^{15}N_{NO_3}$ values range from −0.94‰ to 7‰ (mean 2.71‰) with the $\delta^{18}O_{NO_3}$ values of 4.06‰ to 48.03‰ (mean 21.83‰).

4.4 DOC concentration and $\delta^{13}C_{DOC}$ value

DOC is the main energy source of microbial metabolism in groundwater [15]. The DOC mass concentrations in the karst water ranged from 3.58 to 8.32 mg/L, with from 3.34 to 15.91 mg/L and from 4.06 to 10.55 mg/L for the quaternary pore water and the springs, respectively.

The $\delta^{13}C_{DOC}$ value is an important parameter to indicate the DOC sources and biogeochemical processes. The carbon isotopic compositions of different sources of DOC have different ranges. The average value of δ^{13}C is −25‰ for terrestrial plants, −23‰ for C_3 plants (such as trees, wheat, rice), −13‰ for the C_4 plants (such as corn, sorghum, millet, sugar cane) [16]. The ^{13}C value of soil organic matter was associated with the regional plant type, and was (−27±5)‰ for peat humic soil organic matter, and was up to −40‰ in the serious pollution areas such as landfill [13]. The $\delta^{13}C_{DOC}$ value of groundwater in the study area ranged from −22.39‰ to −32.39‰ with mean value of −27.39‰, which coincided with the ^{13}C value of soil organic matter [16]. As shown in the histogram of δ^{13}C of DOC (Fig. 4), approximately 95% of the samples had $\delta^{13}C_{DOC}$ values between −23‰ and −30‰. There was distinct variation in the isotopic distribution among areas. The $\delta^{13}C_{DOC}$ values of the karst water range from −29.65‰ to −22.8‰ with mean value

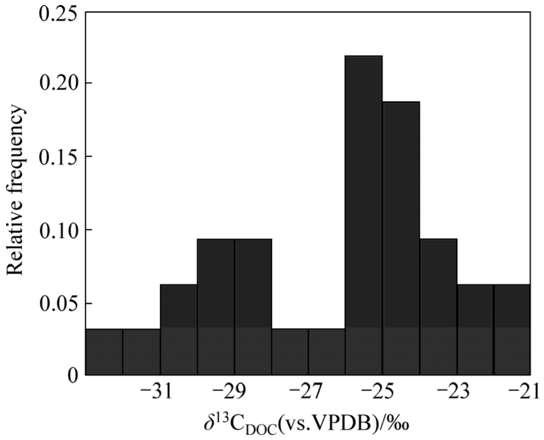

Fig. 4 Relationship between relative frequency and δ^{13}C value of DOC in groundwater in study area

of −26.18‰, while from −31.69‰ to −22.39‰ with mean value of −27.36‰ for the quaternary pore water, and from −26.09‰ to −23.72‰ with mean value of −25.16‰ for the spring water.

5 Discussion

5.1 Transport and transformation of nitrate in groundwater

5.1.1 Indication of chloride and nitrate concentrations

The Cl^- sources in water from various areas generally include natural sources (dissolution of minerals), agricultural chemicals (potash or KCl), animal waste, septic effluent, and road salt [17]. There is some contaminated groundwater, which might indicate that most of the Cl^- was mainly of anthropogenic origin. Chloride is a good indicator of sewage impacts because it is not subjected to physical, chemical, and microbiological processes occurring in groundwater. HO_3^-/Cl^- method can provide more information to distinguish the effect of N removal processed by dilution from denitrification. In this work, there is no positive or negative relationship observed between HO_3^- and Cl^- (Fig. 5), which might indicate that the mixing process had a major effect on nitrate transportation. However, there is a generally negative correlation between HO_3^- and Cl^- in the eastern plain and piedmont plain, which may provide conclusive evidence of the wastewater pollution and denitrification [18]. In the western mountains and hilly region, there is positive relationship observed between HO_3^- and Cl^-, due to the chemical fertilizer inputs. The linearity between nitrate and chloride concentration indicates a common source of nitrate for the groundwater samples HN011, HN020, HN029, HN030 and HN036.

5.1.2 Impact of biogeochemistry on $\delta^{15}N_{NO_3}$ and $\delta^{18}O_{NO_3}$ values

Characterizing biogeochemical process in groundwater is a key issue to understand the source and fate of nitrate in groundwater. DOC is the main energy source of microbial metabolism in groundwater [15]. The $\delta^{13}C_{DOC}$ value is an important parameter to indicate the DOC sources and biogeochemical processes. As indicated by Fig. 6, there is a negative relationship between DOC and $\delta^{13}C_{DOC}$, which accords with a Rayleigh process, in other words, the DOC concentration increases with the $\delta^{13}C_{DOC}$ value decreasing. The $\delta^{13}C_{DOC}$ and $\delta^{15}N_{NO_3}$ values of the groundwater samples show a generally positive correlation, indicating that the biogeochemical processes significantly affected nitrogen isotope composition in the groundwater (Fig. 7), and the same as the $\delta^{13}C_{DOC}$ and $\delta^{18}O_{NO_3}$ values (Fig. 8),which may be caused by these factors. From the point of the biological process, denitrification might occur during runoff due to the bad soil aeration and bad water permeability; therefore, nitrate is taken as electron acceptor due to that fact that the HO_3^- content decreased, and the synthetic of the microbial cells required large amount of DOC, so the DOC concentration is reduced. From the point of isotope, C, N and O isotope fractionation conformed to Rayleigh theory, meaning that the $\delta^{13}C_{DOC}$, $\delta^{15}N_{NO_3}$ and $\delta^{18}O_{NO_3}$ values increase with the residual DOC and HO_3^- concentrations decreasing.

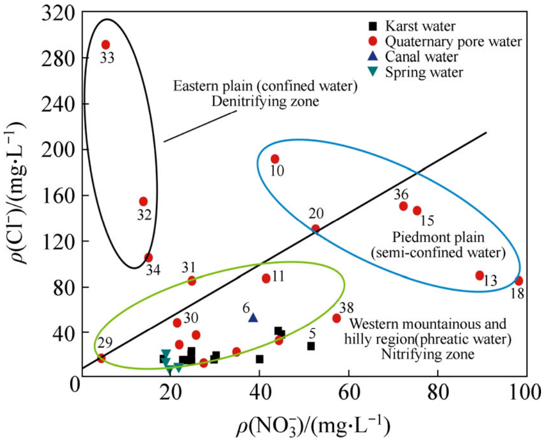

Fig. 5 Plot of stable isotope ratio of Cl^- vs HO_3^- concentration

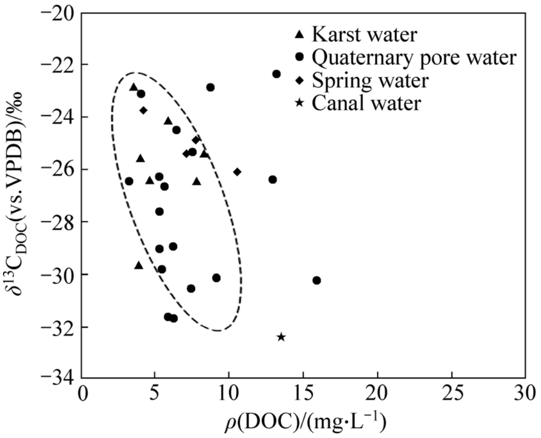

Fig. 6 Plot of $\delta^{13}C_{DOC}$ vs DOC mass concentration

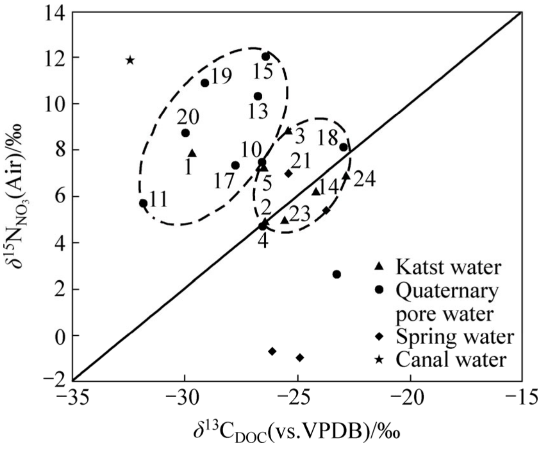

Fig. 7 Plot of $\delta^{13}C_{DOC}$ vs $\delta^{15}N_{NO_3}$

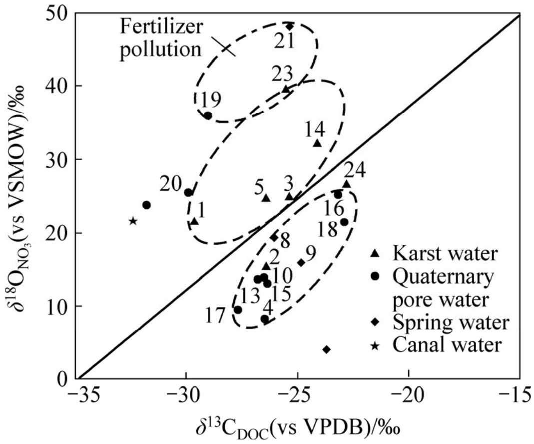

Fig. 8 Plot of $\delta^{13}C_{DOC}$ vs $\delta^{18}O_{NO_3}$

5.2 Identification of nitrate source in groundwater

Groundwater nitrate pollution in Linzhou, Anyang area, may originate from multiple sources, including chemical fertilizer, manure and wastewater, crop residues and other types of organic matter of the soil tillage fields and natural soil (forest and grass), NH_4^+ fertilizer, atmospheric deposition [3]. It has been reported that HO_3^- in atmospheric deposition has $\delta^{15}N$ values in the range of −10‰ to 12‰ [19]. Chemical NO_3^- fertilizers typically have $\delta^{15}N$ values of 12‰, which is close to that of atmospheric N_2 [15, 19]. Many sources of HO_3^- have wide and overlapping ranges of $\delta^{15}N$, and $\delta^{15}N-HO_3^-$ is often modified by isotopic fractionation caused by physical, chemical and microbial processes, such as nitrification, NH_3 volatilization and denitrification. Therefore, the sources and transformations in soil solutions, groundwater and surface water cannot be fully elucidated using only N isotopes [20]. $\delta^{18}O-HO_3^-$ can be useful to identify HO_3^- from atmospherically and microbially produced HO_3^- due to the wide variability in the $\delta^{18}O_{NO_3}$ values between sources [10, 21]. According to the nitrogen and oxygen isotopic composition values from different nitrogen sources reported by SAVARD et al [22] (Fig. 9), the $\delta^{18}O_{NO_3}$ values of ammonium fertilizer, soil organic matter and animal manure are similar, and the $\delta^{15}N$ values are different. The $\delta^{18}O_{NO_3}$ values of atmospheric deposition is up to 50‰−70‰, which is significantly different from other nitrogen sources. The most of groundwater samples in the study area fall into the mixing range, which indicated that the main nitrate source is chemical HO_3^- fertilizer due to the high utilization of farmland and much chemical fertilizer given in the large distribution area, and only a portion of that fall into the soil organic matter range, which indicated that the main nitrate source is soil organic matter. There was only one point (sample 15), with the HO_3^- mass concentration of 75.47 mg/L, 12‰ for $\delta^{15}N_{NO_3}$ and 12.93‰ for $\delta^{18}O_{NO_3}$, the DOC mass concentration of 5.36 mg/L, the $\delta^{13}C_{DOC}$ value of −24.15‰, the well depth of 6 m. We presumed that this results were given due to the contamination of animal manure.

Denitrification is an important mechanism for reduction of the HO_3^- load in aquatic environments via transformation of dissolved HO_3^- to N_2 and N_2O. Denitrification usually causes isotopic enrichment of the residual HO_3^- [2−3]. The extent of fractionation during denitrification is dependent on the fraction of the substrate pool that is consumed [19]. In this work, significant denitrification is found to impact on HO_3^- distribution in the quaternary pore waters (Fig. 9). Additionally, positive interaction is found between $\delta^{15}N_{NO_3}$ and $\delta^{18}O_{NO_3}$ (Fig. 9), which suggests that denitrification/biological process might influence the isotopic values of nitrate due to nitrate with high $\delta^{15}N$ values having high $\delta^{18}O$ values in some waters.

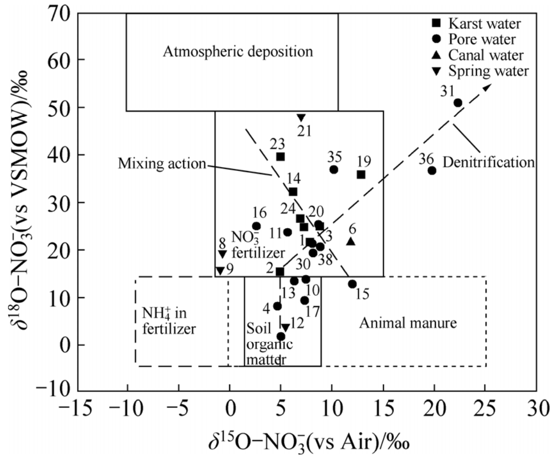

Fig. 9 Plot of $\delta^{18}O-HO_3^-$ vs. $\delta^{15}N-HO_3^-$ in groundwater of study area

The above discussion shows that water denitrification would be significant for fractionating the isotopes of HO_3^-. These findings are similar to those of other studies. BÖTTCHER et al [3] have made an attempt to ascertain the significance of denitrification in specific depth sections at two other multilevel wells using the previously quantified enrichment factors for $\delta^{15}N$ and $\delta^{18}O$ in a sandy aquifer. PANNO et al [23], in a study of the Mississippi River, found that the majority of the denitrication appeared to have occurred in soil or groundwater before discharge into the river. LI et al [10] suggested that denitrification shifts the isotopic values of HO_3^- in the part of the Changjiang River during a long drought. These authors suggest that this should be taken into an account when determining the N budget. MAYER et al [24] gave a detailed explanation of denitrification generating increased $\delta^{15}N$ and $\delta^{18}O$ values; however, the simultaneous addition of HO_3^- from sewage or manure in watersheds with significant urban and agricultural land use would readily mask any isotopic denitrification signal. Obviously, denitrification could occur in the whole basin regardless of the lack of isotopic proof. In the study, some water samples were found to have HO_3^- with high $\delta^{15}N$ and $\delta^{18}O$ values, with samples 31, 35 and 36 having $\delta^{18}O$ values of above 20‰. This suggests that denitrification might occur in some microenvironments within the catchment.

6 Conclusions

1) Agricultural fertilizer is the main source of groundwater nitrate, as well as manure and wastewater.

2) The soil organic matter mainly comes from C_3 plants indicated by $\delta^{13}C_{DOC}$ values. A good positive correlation is observed between $\delta^{13}C_{DOC}$ and $\delta^{18}O_{NO_3}$, which can be used as an important indicator for identification nitrate sources in groundwater.

3) The groundwater recharge area is dominated by mineralization, nitrification and mixing processes, whereas the confined groundwater area is dominated by denitrification processes. In the future, multi-element isotopes and microbial technology is the main trend for the study of nitrate pollution.

References

[1] RIVETT M O, BUSS S R, MORGAN P, SMITH J W N, BEMMENT C D. Nitrate attenuation in groundwater: A review of biogeochemical controlling processes [J]. Water Research, 2012, 42(16): 4215−4232.

[2] ARAVENA R, ROBERTSON W D. Use of multiple isotope tracers to evaluate denitrification in ground water: Study of nitrate from a large-flux septic system plume [J]. Ground Water, 2009, 36(6): 975−982.

[3] BÖTTCHER J, STREBEL O, VOERKELIUS S, SCHMIDT H. Using isotope fractionation of nitrate−nitrogen and nitrate−oxygen for evaluation of microbial denitrification in a sandy aquifer [J]. Journal of Hydrology, 2010, 114(3/4): 413−424.

[4] FUKADA T, HISCOCK K M, DENNIS P F, GRISCHEK T. A dual isotope approach to identify denitrification in groundwater at a river-bank infiltration site [J]. Water Research, 2011, 37(13): 3070−3078.

[5] KAPLAN N, MAGARITZ M. A nitrogen-isotope study of the sources of nitrate contamination in groundwater of the pleistocene coastal-plain aquifer, israel [J]. Water Research, 2006, 20(2): 131−135.

[6] KREITLER C W. Nitrogen-isotope ratio studies of soils and groundwater nitrate from alluvial fan aquifers in texas [J]. Journal of Hydrology, 1979, 42(1/2): 147−170.

[7] MARIOTTI A, LANDREAU A, SIMON B. N-15 isotope biogeochemistry and natural denitrification process in groundwater-application to the chalk aquifer of northern france [J]. Geochimica et Cosmochimica Acta, 1988, 52(7): 1869−1878.

[8] SMITH R L, HOWES B L, DUFF J H. Denitrification in nitrate-contaminated groundwater-occurrence in steep vertical geochemical gradients [J]. Geochimica et Cosmochimica Acta, 1991, 55(7): 1815−1825.

[9] WASSENAAR L I. Evaluation of the origin and fate of nitrate in the abbotsford aquifer using the isotopes of N-15 and O-18 in NO_3^- [J]. Applied Geochemistry, 1995, 10(4): 391−405.

[10] LI Si-liang, LIU Cong-qiang, LI Jun, LIU Xiao-long, CHETELAT B, WANG Bao-li, WANG Fu-shun. Assessment of the sources of nitrate in the changjiang river, China using a nitrogen and oxygen isotopic approach [J]. Environmental Science & Technology, 2010, 44(5): 1573−1578.

[11] KENDALL C, SNIECKUS V. Tracing nitrogen sources and cycling in catchments [C]// KENDALL C, McDONNELL J J. Isotope Tracers in Catchment Hydrology. Amsterdam: Elsevier Science BV, 1998: 519−576.

[12] YANG Yan, CAI He-sheng, LIU Cun-fu, ZHOU Ai-guo. The application of isotopes $\delta^{15}N$ and $\delta^{18}O$ in NO_3^- technique in the study on nitrogen contamination to groundwater in Karsr area−A case study on the high incident region of esophagus cancer in Linzhou, Henan, China [J]. Carsologica Sinica, 2004, 23(3): 206−212.

[13] CRAIG H. Istopic variations in meteoric waters [J]. Science, 1961, 133: 1702-3.

[14] ZHENG S H, ZHANG Z F, NI B L, HOU F G, SHEN M Z. Hydrogen and oxygen isotopic studies of thermal waters in Xizang [J]. Acta Scientiarum Naturalium Universitatis Pekinensis, 2011: 99-106.

[15] THURMAN E M. Organic ceochemistry of natural waters [M]. Dordrecht: Springer Netherlands, 1985.

[16] CLAY D E, CLAY S A, MOORMAN T B, BRIXDAVIS K, SCHOLES K A, BENDER A R. Temporal variability of organic C and nitrate in a shallow aquifer [J]. Water Research, 1996, 30(3): 559−568.

[17] LI Si-liang, LIU Cong-qiang, LI Jun, XUE Zi-cheng, GUAN Jin, LANG Yun-chao, et al. Evaluation of nitrate source in surface water of southwestern China based on stable isotopes [J]. Environ Earth Sci, 2013, 68: 219−228.

[18] LIU Cong-qiang, LI Si-liang, LANG Yun-chao, XIAO Hong-ye. Using $\delta^{15}N$ and $\delta^{18}O$ values to identify nitrate sources in karst ground water, Guiyang, southwest China [J]. Environmental Science & Technology, 2006, 40(22): 6928−6933.

[19] KENDALL C, ELLIOTT E M, WANKEL S D. Tracing anthropogenic inputs of nitrogen to ecosystems [M]. 2nd ed. Oxford: Blackwell, 2007.

[20] MAYER B, BOLLWERK S M, MANSFELDT T, HUTTER B, VEIZER J. The oxygen isotope composition of nitrate generated by nitrification in acid forest floors [J]. Geochimica Et Cosmochimica Acta, 2001, 65(16): 2743−2756.

[21] HALES H C, ROSS D S, LINI A. Isotopic signature of nitrate in two contrasting watersheds of brush brook, vermont, USA [J]. Biogeochemistry, 2007, 84(1): 51−66.

[22] SAVARD M M, SOMERS G, SMIRNOFF A, PARADIS D, van BOCHOVE E, LIAO S. Nitrate isotopes unveil distinct seasonal N-sources and the critical role of crop residues in groundwater contamination [J]. Journal of Hydrology, 2010, 381(1/2): 134−141.

[23] PANNO S V, HACKLEY K C, KELLY W R, HWANG H H. Isotopic evidence of nitrate sources and denitrification in the Mississippi river, Illinois [J]. Journal of Environmental Quality, 2010, 35(2): 495−504.

[24] MAYER B, BOYER E W, GOODALE C, JAWORSKI N A, VAN BREEMEN N, HOWARTH R W. Sources of nitrate in rivers draining sixteen watersheds in the northeastern US: Isotopic constraints [J]. Biogeochemistry, 2002, 57(1): 171−197.

(Edited by DENG Lü-xiang)